

## CONTRIBUTION OF TITANIUM, CHROMIUM AND CARBON BUFFER INTERLAYERS TO BIO-TRIBOLOGICAL PROPERTIES OF MULTILAYER COMPOSITES

Research studies on bio-tribological protective coatings of titanium, chromium and carbon based have been performed. Thin films were fabricated by hybrid PLD technique (PLD supported by magnetron sputtering). Coatings consisted of two parts; the inner part (first from the substrate) in each case was formed by titanium or chromium/ titanium nitride or chromium nitride (Ti/TiN or Cr/Cr<sub>2</sub>N). The outer part was formed by pure DLC or multilayer DLC/Ti or Cr. No delamination was found at the interface. Titanium or chromium metallic layer was deposited as a first layer directly on the metallic substrate to avoid delamination. All individual layers were built of columnar nano- crystallites. Mechanisms of the mechanical wear of analyzed systems were presented, focusing on the cracking propagation in ball-on-disc tests using an 1 N and 5 N applied loads for 5 000 cycles. Complex microstructure analysis of presented nano-multilayer coatings, before and after mechanical tests, were performed by means of transmission electron microscopy (TEM). The highest stress concentration during mechanical uploading was moved through the multilayer coating by breaking only one layer at the time. The microstructure characterization revealed that cracking propagating in the outer part of the coating was stopped at the interface. In the case of the inner part of the coating Ti/TiN; Cr/Cr<sub>2</sub>N, ceramic layers showed brittle cracking, while metallic (Ti or Cr) ones deformed plastically. Fabricated coatings were subjected under the analysis in the biomechanical system optimized to test for the direct contact with a human whole blood. The study considered physiological conditions mainly related to the temperature and humidity and the frequency of cyclic deformation of the artificial vessel into which the tested sample was introduced.

*Keywords:* bio-tribological coatings, wear mechanism, microstructure

### 1. Introduction

Recently much attention in the coatings design has been paid to their multifunctionality [1]. Multilayer coatings can lead to benefits in performance over comparable single-layers and can combine properties of different materials with one protective coating [2–4]. Crack initiation and propagation are often responsible for wear and the removal of coatings. Introduction of a number of interfaces parallel to the substrate surface can act to deflect cracks or provide barriers to the dislocation motion, increasing the toughness and hardness of the coating [5–9]. Despite much research work on the development of multilayer coatings with superior mechanical and tribological properties, a question still remains about the mechanisms, operating at the smallest length scale, underlying the mechanical response [10]. The wear resistance is often attributed to the high hardness as well as to a good chemical stability. Achievement of high hardness ought to be linked with a large number of internal interfaces, which act as sites of energy dissipation and crack deflection. Coatings can be even applied for tribological medical systems, namely for surgical tools. In this field they can be applied to increase hardness, improve wear and corrosion resistance.

The goal of the presented paper was to study wear mechanisms focusing on the role of metal buffer interlayers operating in the small length scale of titanium, chromium and

carbon basis multilayers systems like: Ti/TiN; Cr/CrN and a-C:H/Ti, a-C:H/ Cr.

### 2. Materials and methods

A hybrid Pulsed Laser Deposition (PLD) system (PLD connected with magnetron sputtering) equipped with a high purity titanium (99.9% Ti), chromium (99.9%Cr) and carbon (graphite) targets were used for the multilayer coating deposition. By application of magnetron sputtering in PLD coating plants, higher deposition rates could be reached and a very good film adhesion was achieved even at room temperature. Coatings were produced by the sequential deposition TiN/Ti, CrN/Cr and amorphous carbon a-C:H/TiN layers. Pure Ti and Cr layers were deposited in an argon (non-reactive) atmosphere, while for the TiN or CrN deposition the atmosphere was gradually switched to nitrogen. To increase the quality of the coating adhesion and to reduce the residual stress concentration, the thin metallic titanium (Ti) or chromium (Cr) layers were deposited as buffer layers at each interface. Details of the deposition process have been described elsewhere [11]. The set of multilayer coatings with a different number of layers and phase ratios at constant total coating thicknesses (1.5 μm) were produced. The coating microstructure was studied by means of a TECNAI G2 F20

\* INSTITUTE OF METALLURGY AND MATERIALS PAS, 25 REYMONTA STR., 30-059 KRAKÓW., POLAND

\*\* JOANNEUM RESEARCH, MATERIALS –INSTITUTE FOR SURFACE TECHNOLOGIES AND PHOTONICS, LEOBEN, AUSTRIA

<sup>#</sup> Correspondence author: l.major@imim.pl

FEG (200 kV) transmission electron microscope (TEM). Chemical analysis was performed using energy dispersive X-ray spectroscopy (EDS). Thin foils for microstructure observations were prepared using a QUANTA 200 3D dual beam focused ion (FIB) equipped with an OmniProbe in-situ lift out system.

The mechanical properties of the coatings were investigated by means of nano-indentation (Berkovich indenter) and a ball-on-disc mechanical test using 5 N applied loads for 20 000 cycles. All mechanical tests were performed in natural atmosphere (in air).

An Al<sub>2</sub>O<sub>3</sub> alumina ball with 6 mm diameter was used for the test. The linear speed of the ball, which was applied in the test was 0.06 m/s. Both tests' parameters are presented below:

- Low stress condition: Load  $F = 1$  [N]; ball radius  $R = 3$  [mm]; cycle number  $n = 20.000$ ; friction radius  $r = 5$  [mm], linear speed  $v = 0.06$  [m/s]; nanohardness  $H = 0.45$  [GPa].
- High stress condition: Load  $F = 5$  [N]; ball radius  $R = 3$  [mm]; cycle number  $n = 5.000$ ; friction radius  $r = 4$  [mm], linear speed  $v = 0.05$  [m/s]; nanohardness  $H = 0.8$  [GPa].

Bio- medical tests were done using smooth muscle cells. 12,13 Smooth muscle cells (SMC) were purchased from Lonza. Each vial had a concentration of 500 000 cells/mL. The cells were stored in liquid nitrogen until use. Before adding cells, the medium was warmed at 37°C in a water bath. Cells were taken from the liquid nitrogen container and placed for 2–3 min into a 37°C water bath. SMC were deposited directly on the surfaces of coatings. After three days the cells were fixed in 4 % paraformaldehyde. Then the cells were permeabilised in a detergent Triton X-100 0.2 % for 4 min. The actine cytoskeleton was marked with AlexaFluor Phalloidin, the nucleus with DAPI. Fluorescent dyes were excited with appropriate laser wavelength, 488 nm for actin cytoskeleton visualization, 405 nm to visualize nucleus of the cell. The cells adhesion to the coatings surfaces were observed by confocal microscopy (Carl Zeiss Exciter 5).

The cytotoxic effect was determined according to the ISO 10993-5:2009 standards. 23 Samples in size of 1.5 cm<sup>2</sup> were placed in confluent mouse fibroblast (L929; ATCC) cultures (about 5 \_ 10<sup>5</sup> cells) and were incubated for 48 hours at 37 deg.C. Then cells were stained by propidium iodide (PI). Cultures incubated with the samples were analyzed in comparison with control cultures. Images were taken with the Exciter 5 confocal microscope equipped with a camera, and quantified using AxioVision 4.8 software (Carl Zeiss MicroImaging). A statistical analysis (two-way ANOVA and Tukey's post hoc test, P value smaller than 0.05 was considered as significant – Statistica 10.0 PL) was performed on three replicates from each treatment.

### 3. Results

#### 3.1. Microstructure analysis of as deposited TiN/Ti/a-C:H coatings

The main goal of the examinations was to establish the bio-tribological multilayer TiN/Ti/a-C:H coatings and to describe the microstructure changes and wear mechanisms

operating at the small length scale of the described multilayer coatings after mechanical uploading. The microstructure characterization has been performed on as-deposited coatings, as well as on those after mechanical wear test to observe changes in the microstructure caused by mechanical uploading. To improve the adhesion of the coating to the substrate, a titanium (Ti) metallic buffer layer was deposited as the first one. Subsequently an appropriate multilayer structure was produced, where carbon layers were placed sequentially with titanium nitride layers (Fig. 1)(Fig. 2).

The list of different coatings architecture is presented below:

- a-C:H single layer
- TiN single layer
- 2xTiN/a-C:H (4 layers with TiN to a-C:H phases ratio 1:1)
- 8xTiN/a-C:H (16 layers with phases ratio 1:1)
- 32xTiN/a-C:H (64 layers with phases ratio 1:1)
- 8xTiN/a-C:H (16 layers with phases ratio 1:2)
- 8xTiN/a-C:H (16 layers with phases ratio 1:4)
- 8xTiN/a-C:H (16 layers with phases ratio 4:1)

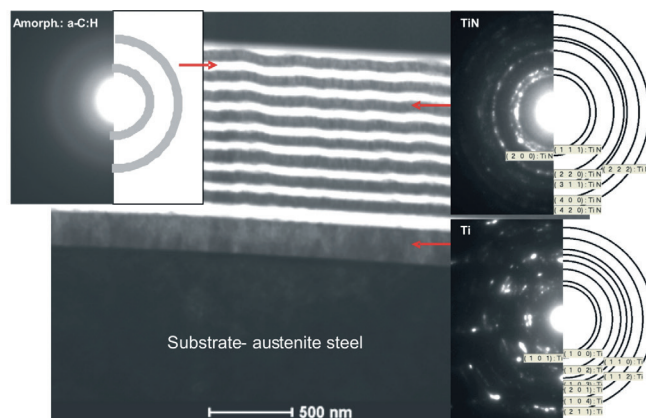


Fig. 1. TEM bright field image of an as-deposited 8 TiN/Ti/a-C : H multilayer coating, together with selected area electron diffraction patterns from selected parts of the coating

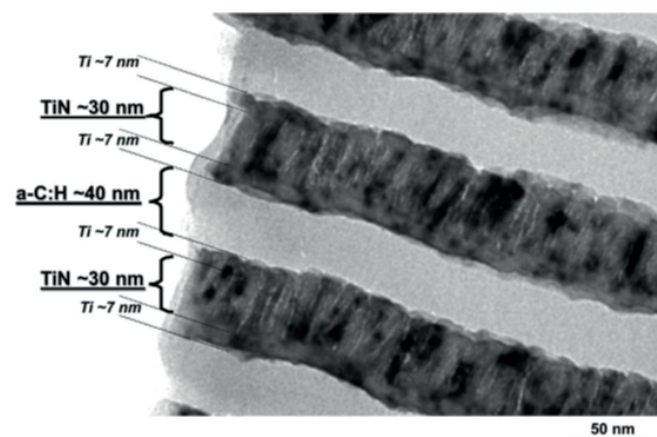


Fig. 2. TEM bright field image of an as-deposited 8 TiN/Ti/a-C : H multilayer coating; higher magnification than Fig.1, revealing thin Ti layers presented at each interface

The small amount of the Ti phase between the TiN and a-C : H layers improves the adhesion of TiN to a-C : H,

which otherwise would be very weak due to a high residual stress. The thickness of the individual titanium layers was approximately 7 nm. The presence of the metallic titanium phase was confirmed by the EDS qualitative chemical analysis and the HRTEM technique in the atomic scale (Fig. 3). The above observations correspond to the deposition process. The pure titanium layers were deposited in an argon atmosphere. As a result, a very thin titanium phase was formed at each TiN/a-C : H interface. The atmosphere was subsequently switched to a mixture of argon and nitrogen. The nitrogen flow was gradually opened while the argon flow was closed. After reaching the half thickness of the TiN layer, the nitrogen flow was gradually closed, and the argon flow was opened. Similar to before, deposition from the Ti target was finished in an argon atmosphere, allowing the formation of a small amount of Ti phase on the next TiN/a-C : H interface. Concerning only the TiN phase in the layer, the Ti to N ratio was changed with the distance from the interface. It happened because the gases flow changed with the distance from the interface. The flow was gradually changed.

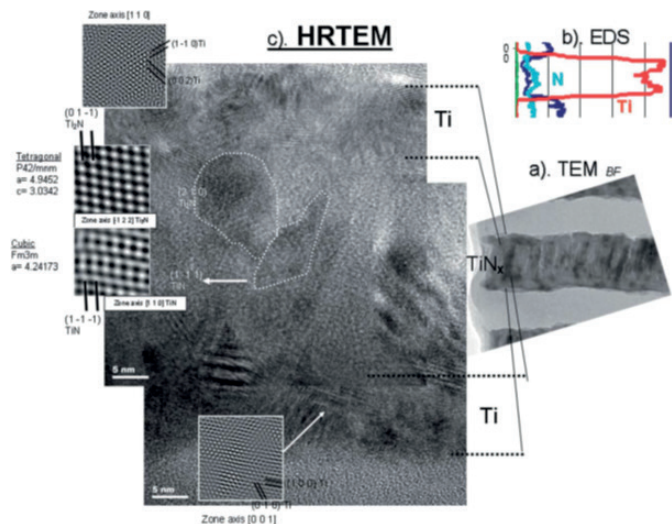


Fig. 3. HRTEM image of the one Ti/TiN/Ti parts of the coating; (a) bright field image of the one Ti/TiN/Ti fragments of the coating, (b) STEM/EDS line analysis of elements distribution, (c) HRTEM image of the analyzed part

### 3.2. Microstructure analysis of TiN/Ti/a-C : H coatings after mechanical test

The second step of the microstructure characterization comprised the analysis of the cross-section of the TiN/Ti/a-C : H multilayer coatings after the mechanical wear test. A detailed analysis of the wear mechanisms have been done by the TEM method. One of the main advantages of the described coatings was that cracking had not been performed suddenly. It occurred layer by layer (Fig. 4). The highest, localized stress concentration was moved during the coating deformation from the bottom to the top part of the coating. The layers reunion after movement of individual layers to the closest layer of the same phase was possible by the presence of metallic thin buffer layers at each interface.

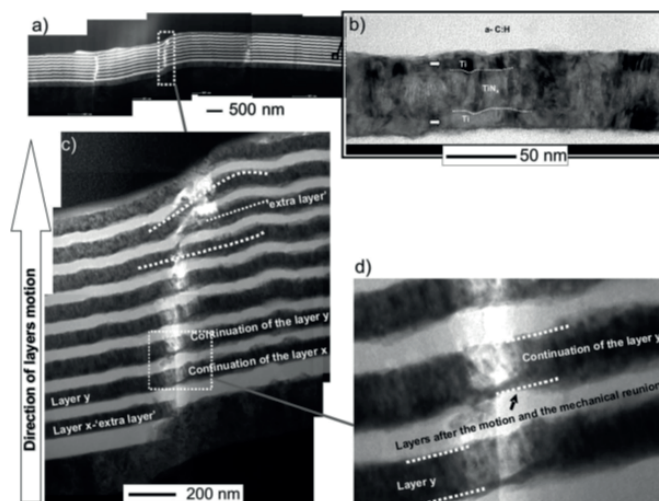


Fig. 4. TEM bright field image of the cracking place in an 8 TiN/Ti/a-C : H coating (cross section): (a) TEM bright field image of the cracked place, (b) image revealing presence of thin Ti metallic layers at each TiN/a-C : H interface, (c) the magnified area of one crack presenting the 'layers motion mechanism', (d) place of layers reunion after 'layers motion'

### 3.3. Investigation of wear resistance

At the low stress condition of the ball-on-disc test, wear indexes for multilayer coatings were between indexes for single layer coatings. The lowest wear was found for the a-C : H single layer coating (Fig. 5a). In the high stress condition the role of the multilayer structure started to be visible. Wear indexes for multilayer coatings were on the same level or even lower than index for the a-C : H single layer coating (Fig. 5b).

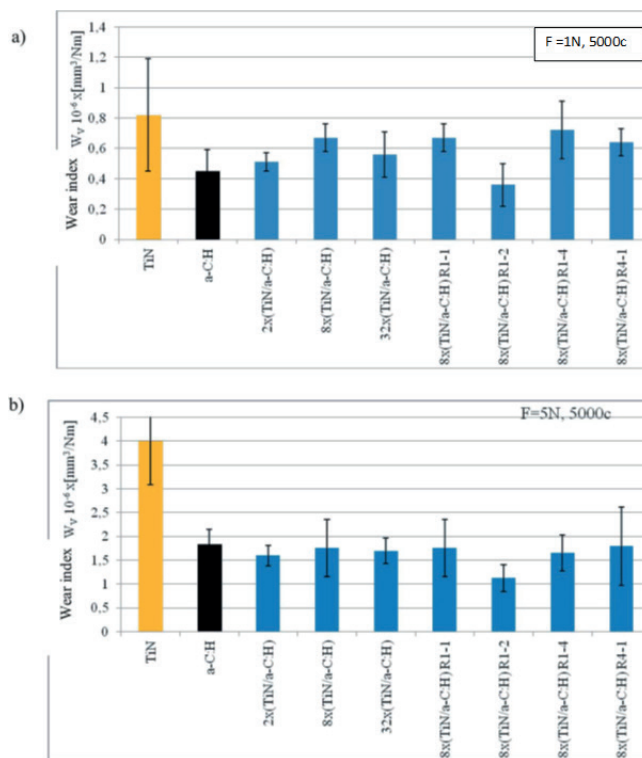


Fig. 5. Wear (ball-on-disc) test results: (a) low stress condition (1 N), (b) high stress condition (5 N)

### 3.4. Smooth muscle adhesion test

Medical tools (like tweezers) by contacting with vessels have the first contact with smooth muscle cells. The bio-test with these cells was treated as a criteria for the best multilayer coating selection for microstructure characterizations. The best cell-material interaction adhesion was found for the 8 TiN/Ti/a-C:H coating (Fig. 6).

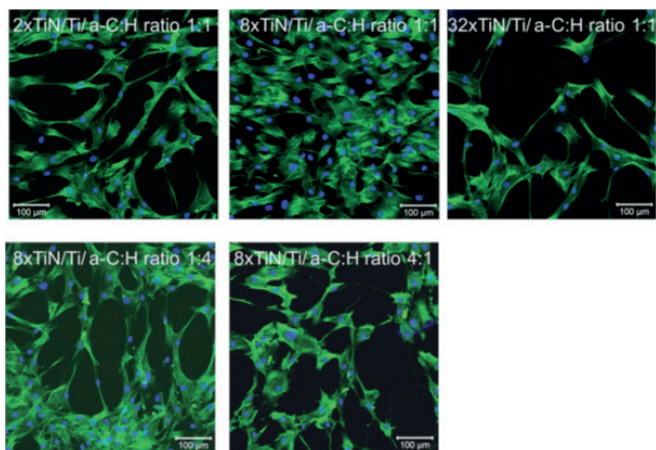


Fig. 6. Smooth muscle cell adhesion observed by confocal microscopy

### 4. Bio-tribological Cr/CrN + a-C:H nanomultilayer protective coatings for carbon–fiber composite materials

Carbon–carbon (C/C) composites or carbon–fiber-composites (CFC) are increasingly being considered for aerospace application. In composite materials, the fibers impart strength, stiffness and fatigue resistance, while the carbon matrix holds the fibers. Carbon-based materials show, however, significant oxidative degradation in air beginning at temperatures in the region of 400 degC. Therefore, a coating concept for carbon–carbon composites consists of an inner part, which serves as a structural link with stress compensation ability to the carbon substrate, and an outer part, which acts as a diffusion barrier. Basing on the earlier studies on Ti/TiN and Cr/CrN coatings [12–18], the chromium/chromium nitride (Cr/CrN) multilayer structure has been selected as the inner part. The outer part of the coating, in the present paper, was hydrogenated amorphous carbon (a-C:H). Coatings were deposited by means of magnetron sputtering technique. Mechanisms of a mechanical wear of analyzed systems were presented, focusing on the cracking propagation in ball-on-disc tests using 1 N and 5 N applied loads for 5 000 cycles. Complex microstructure analysis of presented nano-multilayer coatings, before and after mechanical tests, were performed by means of TEM.

Structure, microstructure and nanostructure are critical aspects for surface engineering [19]. Microstructure characterization of the as deposited protective multilayer coating, described in the presented paper, was characterized mainly using TEM. Thin foils for TEM observation have been cut using FIB perpendicular to the carbon fibers. No delamination was noticed. The coating clearly reflects the surface roughness of the carbon–fiber composite (CFC) substrate. The subjected to analyze coating contained two

parts. The Cr/CrN (chromium/chromium nitride) multilayer which was deposited as a first part from CFC substrate (inner part). The second part was amorphous carbon (a-C:H). The purpose of the Cr/CrN part was to reduce residual stress of total coating, especially at the substrate/coating interface, as well as to enhance coating adhesion to CFC substrate. Because of the presence of a metallic phase (chromium – Cr), total coating had partially plastic properties. Such behavior has been described by the authors in previous papers [12–14] as well as by other researchers [20]. The CrN and Cr lattice parameters allow a cube-on-cube close to epitaxial growth with a low mismatch (1.6%) (Fig. 7) [21].

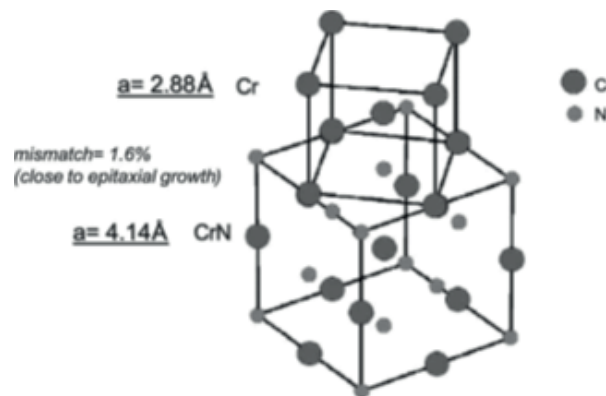


Fig. 7. The scheme of the Cr and CrN cell growth assembly

In the present case, the same diffraction contrast went through interfaces. It confirmed crystallographic dependence between Cr and CrN phases. High resolution analysis of the TEM technique (HRTEM), allowed us to established the mismatch between Cr and CrN. It has been confirmed that the mismatch was on the level of 2.4 deg. Even such a good lattice fit caused formation of defects in the form of mixed dislocations in the structure of the metallic phase (Cr) (Fig. 8). It has been also confirmed that CrN was presented as a Cr<sub>2</sub>N. The presence of defects in the form of dislocations can affect the strengthening of the structure of the metallic phase, which can impact positively on the mechanical properties of the whole coating [22]. The second part of the coating, as it was mentioned at the beginning, formed a multilayer structure built of hydrogenated amorphous carbon (a-C:H) (the other part of the total coating) (Fig. 9).

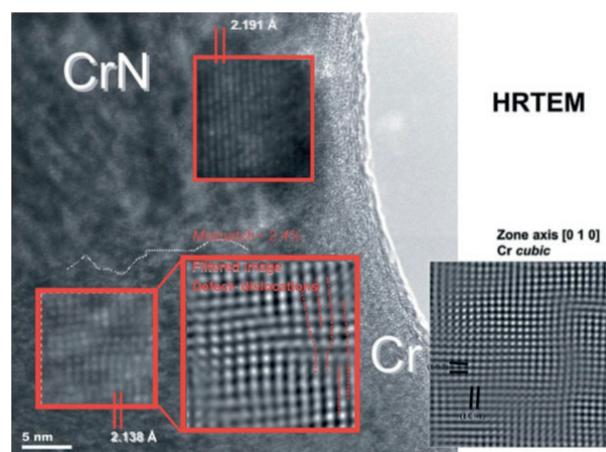


Fig. 8. The HRTEM image of the Cr/CrN interface

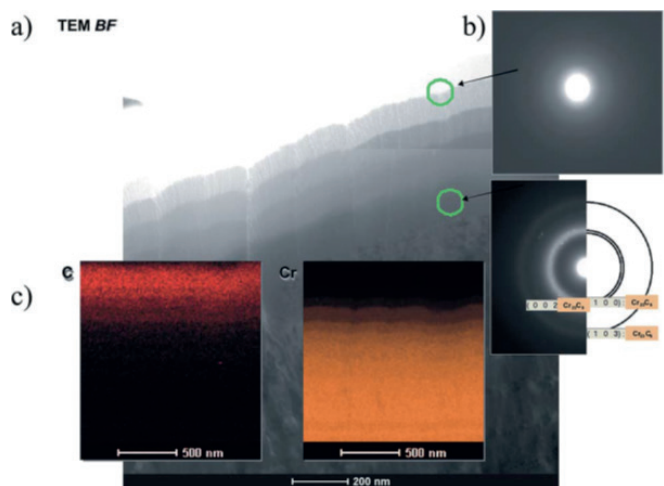


Fig. 9. Microstructure characterization of the amorphous carbon part of the coating (outer part) using TEM technique; (a) TEM BF image; (b) selected area electron diffraction patterns (phase analysis); (c) STEM/ EDS elemental distribution maps

#### 4.1. Microstructure characterization of the Cr/Cr<sub>2</sub>N + a-C:H + Cr nano multilayer coating deposited on carbon fiber composite material, after mechanical tests

Thin foils for TEM characterization were prepared directly from wear tracks using FIB technique. Only this technique allows preparation of thin foil for TEM and getting microstructure information in TEM precisely from the place of interest (in this case from the wear track). At first, changes in microstructure caused by the higher uploading was characterized. The 5 N test is too much for such a sophisticated, very thin coating, but interesting was the fact how this type of coating acted under the pressure of such a large mechanical load [18]. The cross-section of the coating after the 5 N test has been presented in the TEM bright field (TEM BF) image. The coating was seriously destroyed and fragmented, however, it was still present on the substrate, fulfilling its protective role (Fig. 10).

The Cr/Cr<sub>2</sub>N part of the coating played an important role in the cracking protection process. Cr<sub>2</sub>N ceramic layers brittle cracked, while metallic Cr deformed plastically, reducing the cracking energy (Fig. 11). Plastic deformation in metallic Cr layers was realized at 45deg, a typical angle for plastic deformation of polycrystalline, metallic materials [19]. During a wear process, the coating was cracked and fragmented, then parts of the coating were removed in the form of wear debris. In the next step of the wear, the removed material was crushed, mixed together and deposited again on the top of the coating forming so called tribo-film.

The phase analysis of the tribo-film, which was performed using SAED patterns, indicated the presence of chromium nitride and carbon in the form of graphite [18] which is a very good lubricant [20]. Formation of this material during wear is an advantage, which may reduce the friction coefficient. The applied 5 N and 20 000 cycles wear test (ball-on-disc) was too much for such a type of coating; however as it was proved, even under such high uploading conditions, the coating still fulfilled its role. The suitable uploading for such a type of coatings was 1N. The 1 N and 20 000 cycles wear test was performed. After the test, the changes in microstructure have been characterized

using TEM. Looking at the coating microstructure on the cross-section, it has been found that the coating was not so seriously destroyed (Fig.10).

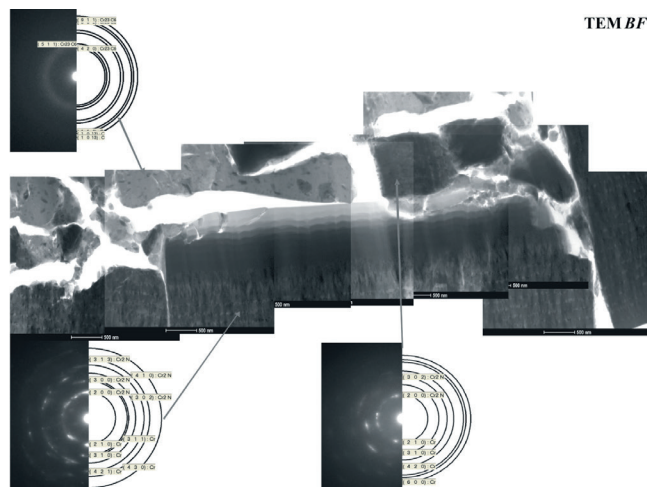


Fig. 10 TEM BF image of the coating after 5 N and 20 000 cycles wear test

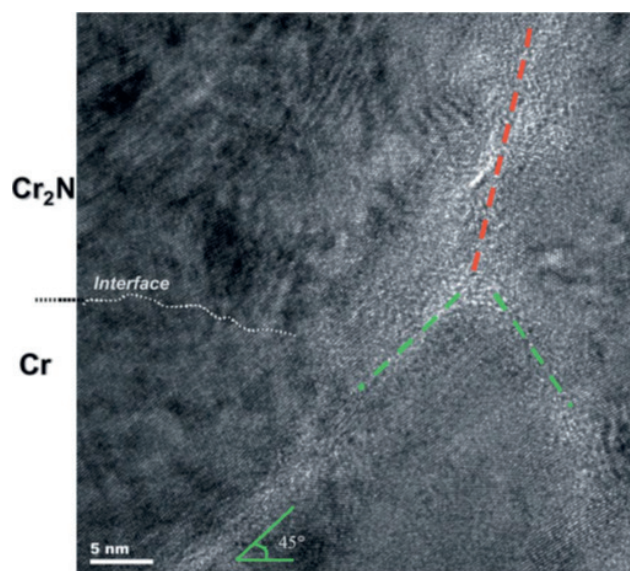


Fig. 11. HRTEM image of the Cr/Cr<sub>2</sub>N interface

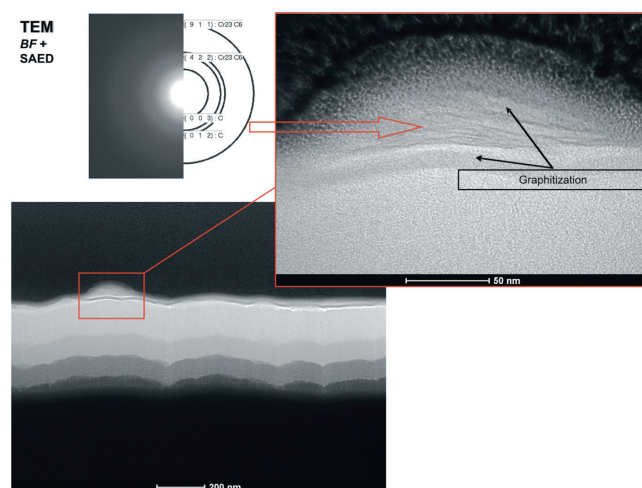


Fig. 12. Microstructure characterization of the tribo-film formed after 1 N and 20 000 cycles wear test, performed by TEM technique

Focusing on the surface topography, it was noticed that at the top of the coating, graphite was formed during the wear process (Fig. 12). The phase analysis performed by diffraction pattern, showed the presence of graphite and chromium carbides in the tribo-film as well. The results were confirmed by high resolution TEM technique [18,23].

#### 4.2. Cytotoxic analysis

Microstructure should influence the induction of inflammatory reactions that can start a rejection reaction or, in the case of medical tools, complications in surgery. The analysis revealed changes dependent on applied deposition parameter. The applied fluorescent marker (PI) is a colorant dye of the nuclei. It cannot penetrate the cell membrane of continuously living cells. Therefore, dead cells are stained. It penetrates into the interior of dead cells through cell membranes damaged in the process of necrosis and intercalates with DNA helix, emitting red light fluorescence (excitation 535 nm, emission 617 nm). The microstructure characterization revealed that cracking, which was propagating in the outer part of the coating (in the carbon part) was stopped at the interface. In the case of the inner part of the coating (Cr/Cr<sub>2</sub>N), ceramic layers showed brittle cracking, while metallic (Cr) ones deformed plastically.

#### 5. Discussion

In general, the layered structure can be vulnerable to failure due to a heterogeneous stress field and reduced toughness at the interfaces. Failures in layered structures could be complicated due to an elastic and toughness anisotropy. Residual stress and elastic mismatch could lead to mixed-mode loading for cracks on and off the interface, as presented by Shaw, Rice, Fleck and Ritchie [14–17]. Elastic/plastic deformations led to microcracking, providing a mechanism for subsequent wear through surface delamination as described by Luo [6]. For cracking of the conventional multilayer system to take place, all the individual layers would need to be broken at the same time. It is suggested that cracking can be controlled by a crack-healing ability or by a plastic deformation and strong interfaces [18–20]. Development of a new generation of coatings, which had both passive mechanical characteristics originated from the matrix material and active response sensitive to change in the local environment, which allowed the fabrication of the future high-tech functional surfaces [21].

In the described experiment, to reduce the high residual stress, a metallic buffer layer of 7 nm was deposited at each TiN/a-C : H interface. Such a composition caused the unusual behavior of the multilayer coating during the mechanical wear, in particular the cracking process. The cracking line, in the described case, because of the presence of very thin Ti layers at each interface, could move through the multilayer coating in the direction of the applied stress by breaking only one layer at a time. Individual layers broke, moved and formed new connection with its neighbour. The mechanism has never been described before in the literature. The layers reunion probably was carried out by moving one broken layer relative to the other along a common interface (in this case-cracking line), while

applying a compressive force. The friction heating generated at the interface softens both components, particularly plastically deformed thin Ti layers presented at each interface. The relative motion was then stopped. The connections were formed in the solid state. Anyway, the ‘layers motion’ phenomenon is similar to the edge dislocation motion (Fig. 10) [22,23]

#### 6. Conclusion [3]

- Multilayer structure and metallic interlayers in the TiN/Ti/a-C : H coatings play major roles in controlling the deformation process.
- Propagation of the deformation was realized layer by layer.
- The cracking line, due to the presence of very thin Ti layers at each interface, could move through the multilayer coating in the direction of the applied stress by breaking only one layer at a time.
- Quality of deposited Cr/CrN + a-C:H + Cr nano multilayer coatings was very high.
- Coatings clearly reflect the surface roughness of the carbon–fiber-composite (CFC) substrate.
- The same diffraction contrast went through interfaces in the Cr/Cr<sub>2</sub>N part of the coating, which confirmed crystallographic dependence between Cr and Cr<sub>2</sub>N phases.
- In the current work, Cr nano-grains have been utilized to modify the structure and properties of amorphous carbon—the second part of the coating; Cr nano-grains were gradually inserted into the carbon structure.
- After 5 N and 20 000 cycles wear test (ball-on-disc), coating was seriously destroyed and fragmented; however, it was still present at the substrate, fulfilling its protective role.
- Cr inserted into amorphous carbon reacted with carbon forming chromium carbides nano-particles (Cr<sub>23</sub>C<sub>6</sub>).
- The HRTEM image presented that a crack propagating through a a-C:H layer with lower Cr<sub>23</sub>C<sub>6</sub> nanoparticles content has been stopped at the interface with another layer of a-C:H with higher amount of Cr<sub>23</sub>C<sub>6</sub>.
- The Cr/Cr<sub>2</sub>N part of the coating also played an important role in cracking protection process. Cr<sub>2</sub>N ceramic layers brittle cracked, while metallic Cr deformed plastically, reducing the cracking energy.
- The 1 N and 20 000 cycle wear test did not cause serious distortion of the coating. No cracks were found. At the surface of the graphite coating, a perfect lubricant was formed.
- The lowest cytotoxic effect was found for the coating deposited according to the “A” variant of deposition.
- Deposition current and adequate gas flow during coatings production may have an influence on their bio-compatible properties.

#### Acknowledgements

Research Project (National Science Centre): Multilayered, wear resistant, self-healing, protective coatings

elaboration for carbon fiber composite materials. Number: 2012/06/M/ST8/ 00408. Research Project (National Science Centre): Biomechanical and microstructure analysis of multilayer nanocomposite, protective coatings for metallic substrates for tissue interaction. Number: 2012/07/B/ST8/03396.

## REFERENCES

- [1] Y. Brechet, J. D. Embury, *Scr. Mater.* **68**, 1–3 (2013).
- [2] Q. Luo, S. Cai Wang, Z. Zhou, L. Chen, *J. Mater. Chem.* **21**, 9746–9756 (2011).
- [3] J. Morgiel, L. Major, B. Major, J.M. Lackner, L. Nistor, *J. Microsc.* **223**, 237–239 (2006).
- [4] 3923–3930 (2008).
- [5] S. Kumar, D. Zhou, D. E. Wolfe, J.A. Eades, M. A. Haque, *Scr. Mater.* **63**, 196–199 (2010).
- [6] Q. Luo, W. M. Reinforth, W.-D. Muenz, *Scr. Mater.* **45**, 399–404 (2001).
- [7] Q. Luo, W. M. Reinforth, W. D. Muenz, *Wear* **225–229**, 74–82 (1999).
- [8] L. Major, W. Tirry, G. Van Tendeloo, *Surf. Coat. Technol.* **202**, 6075–6080 (2008).
- [9] J.M. Lackner, L. Major, M. Kot, *Bull. Pol. Acad. Sci.: Tech. Sci.* **59**, 343–355 (2011).
- [10] P. Goodhew, *Nano Today* **1**, 40–43 (2006).
- [11] J.M. Lackner, W. Waldhauser, R. Ebner, *Surf. Coat. Technol.* **188–189**, 519–524 (2004).
- [12] R. Major, F. Bruckert, J. M. Lackner, W. Waldhauser, M. Pietrzyk, B. Major, *Bull. Pol. Acad. Sci.: Tech. Sci.* **56**, 223–228 (2008).
- [13] L. Major, J.M. Lackner, B. Major, *RSC Advances* **4**, 21108–21114 (2014).
- [14] L. Major, *Arch. Civ. Mech. Eng.* **14**, 615–621 (2014).
- [15] L. Major, J.M. Lackner, M. Kot, M. Janusz, B. Major, *Bull. Pol. Acad. Sci.: Tech. Sci.* **62**, 565–570 (2014).
- [16] M. Kot, L. Major, K. Chronowska-Przywara, J.M. Lackner, W. Waldhauser, W. Rakowski, *Materials and Design* **56**, 981–989 (2014).
- [17] L. Major, M. Janusz, M. Kot, J. M. Lackner, B. Major, *RSC Advances* **5**, 9405–9415 (2015).
- [18] L. Major, W. Tirry, G. Van Tendeloo, *Surf. Coat. Technol.* **202**, 6075–6080 (2008).
- [19] G. Van Tendeloo, D. Van Dyck, S. J. Pennycook, *Handbook of Nanoscopy*, Copyright Wiley-VCH, 2012.
- [20] P. Wicinski, J. Smolik, H. Garbacz, K. J. Kurzydowski, *Thin Solid Films* **519**, 4069–4073 (2011).
- [21] J. Romero, J. Esteve, A. Lousa, *Surf. Coat. Technol.* **188–189**, 338–343 (2004).
- [22] E. Harry, A. Rouzand, P. Juliet, Y. Paleau, *Thin Solid Films* **342**, 207–213 (1999).
- [23] M.C. Shaw, *Eng. Fract. Mech.* **61**, 49–74 (1998).
- [24] J.R. Rice, *J. Appl. Mech.* **55**, 98–103 (1988).
- [25] N.A. Fleck, J. W. Hutchinson, S. Zhigang, *Int. J. Solids Struct.* **27**, 1683–1703 (1991).
- [26] R.O. Ritchie, R.M. Cannon, B.J. Dalgleish, R.H. Dauskardt, J.M. McNaney, *Mater. Sci. Eng., A* **166**, 221–235 (1993).
- [27] E. Harry, A. Rouzand, P. Juliet, Y. Paleau, *Thin Solid Films* **342**, 207–213 (1999).
- [28] J. Romero, J. Esteve, A. Lousa, *Surf. Coat. Technol.* **188–189**, 338–343 (2004).
- [29] Q. Wang, F. Zhou, X. Ding, Z. Zhou, C. Wang, W. Zhang, L. K.-Y. Li, S.-T. Lee, *Tribol. Int.* **67**, 104–115 (2013).
- [30] J. Weertman, J. R. Weertman, *Elementary Dislocation Theory*, Oxford University Press, 1992.
- [31] X. Songa, F. Hofmanna and A. M. Korsunskya, *Philos. Mag.* **90**, 3999–4011 (2010).

